

# Quadratic formula for determining the drop size in pressure-atomized sprays with and without swirl

T.-W Lee, and Keju An

Citation: *Physics of Fluids* **28**, 063302 (2016); doi: 10.1063/1.4951666

View online: <http://dx.doi.org/10.1063/1.4951666>

View Table of Contents: <http://aip.scitation.org/toc/phf/28/6>

Published by the *American Institute of Physics*

---

## Articles you may be interested in

[High fidelity simulation and analysis of liquid jet atomization in a gaseous crossflow at intermediate Weber numbers](#)

*Physics of Fluids* **28**, 082101 (2016); 10.1063/1.4959290

[Puddle jumping: Spontaneous ejection of large liquid droplets from hydrophobic surfaces during drop tower tests](#)

*Physics of Fluids* **28**, 102104 (2016); 10.1063/1.4963686

[Nonlinear dynamics of a thin liquid film deposited on a laterally oscillating corrugated surface in the high-frequency limit](#)

*Physics of Fluids* **28**, 112101 (2016); 10.1063/1.4965819

[On the accuracy of RANS simulations with DNS data](#)

*Physics of Fluids* **28**, 115102 (2016); 10.1063/1.4966639

[Weakly nonlinear instabilities of a liquid ring](#)

*Physics of Fluids* **28**, 114104 (2016); 10.1063/1.4966976

[Linear and nonlinear dynamics of an insoluble surfactant-laden liquid bridge](#)

*Physics of Fluids* **28**, 112103 (2016); 10.1063/1.4967289

---



**COMPLETELY  
REDESIGNED!**

**PHYSICS  
TODAY**

*Physics Today* Buyer's Guide  
Search with a purpose.

## Quadratic formula for determining the drop size in pressure-atomized sprays with and without swirl

T.-W Lee<sup>a)</sup> and Keju An

*School of Engineering for Matter, Transport and Energy, Arizona State University, Tempe, Arizona 85287-6106, USA*

(Received 15 February 2016; accepted 3 May 2016; published online 1 June 2016)

We use a theoretical framework based on the integral form of the conservation equations, along with a heuristic model of the viscous dissipation, to find a closed-form solution to the liquid atomization problem. The energy balance for the spray renders to a quadratic formula for the drop size as a function, primarily of the liquid velocity. The Sauter mean diameter found using the quadratic formula shows good agreements and physical trends, when compared with experimental observations. This approach is shown to be applicable toward specifying initial drop size in computational fluid dynamics of spray flows. *Published by AIP Publishing.* [<http://dx.doi.org/10.1063/1.4951666>]

### NOMENCLATURE

$A$	= cross-sectional area of the spray where drop properties are evaluated.
$A_{\text{inj}}$	= injector exit area
$d_{\text{inj}}$	= injector diameter
$D$	= drop diameter
$D_i$	= drop diameter for the $i$ -th size bin
$D_{32}$	= SMD = Sauter mean diameter
$K, K'$	= proportionality constants for the viscous dissipation term
$n$	= drop number density
$p(D)$	= normalized drop size distribution function
$u_{\text{inj}}$	= mean injection velocity
$\bar{u}$	= mean drop velocity
$\left(\frac{\partial u}{\partial y}\right)$	= average velocity gradient in the spray
$V$	= volume of the spray bounded by $A$ and spray length
$\mu$	= liquid viscosity
$\rho_g$	= ambient gas density
$\rho_L$	= liquid density
$\sigma$	= surface tension

### INTRODUCTION

Determination of the drop size and velocity statistics from sprays is a long-standing problem in two-phase fluid mechanics. From an engineering standpoint, they are important for the obvious reasons of influencing the subsequent vaporization and combustion processes. In practical combustion devices, the fuel is injected in the liquid form and then burned. For this reason, atomization is an integral element in combustion science and engineering. For modeling and computations of spray combustion, the spray drop size and velocities are the starting points.<sup>1</sup> A vast number of works

<sup>a)</sup> Author to whom correspondence should be addressed. Electronic mail: [attwl@asu.edu](mailto:attwl@asu.edu). Department of Mechanical and Aerospace Engineering, Arizona State University, Tempe, Arizona 85287, USA.

exist in empirical modeling, experimental measurements, and computational simulations of drop size and velocity distributions in various spray configurations (a small set of representative works can be found in Refs. 1–19). More recent work Villermaux and co-workers (e.g., Ref. 27) illustrates the dynamical process during spray atomization including ligament formation and their break-up into droplets. Gorokhovski and Herrmann<sup>28</sup> have made advances into resolving detailed structure of atomizing sprays using quasi-direct numerical simulations (DNS) however in that work, they also cite the need for simpler, computationally efficient, phenomenological model for realistic Reynolds and Weber number sprays. Some of the models they suggest, such as stochastic scaling, liquid jet depletion, and liquid surface density modeling,<sup>28</sup> include several components that are currently being investigated for verification and application in spray systems.

Recently, we presented a new, alternate framework for calculating the drop size distribution and velocities, based on the integral form of the conservation equations of mass, momentum, and energy.<sup>20–22</sup> In this approach, the conservation equations for spray flows, after some algebraic work, render themselves solvable through iterative methods. The key is to use the integral form of the conservation equations so that the input injection parameters are related to the output spray parameters, without having to resolve the details of the atomization physics. This is a departure from existing methods, where conservation laws are applied in an integral form between “asymptotic” states, therefore bypassing the need for detailed modeling nor complex set of assumptions. Validations of the solutions have been provided in our previous works,<sup>20–22</sup> and this method is viable in solving for the drop size and velocities. Both the mean drop and size distributions, obtained using the current method, agree well with experimental data.<sup>20</sup> In this work, we present some new results incorporating an updated form for the viscous dissipation term, which leads to a closed-form quadratic equation and formula for predicting the Sauter mean diameter (SMD), and compare with experimental data and correlations for sprays with and without swirl. This method can be adopted for specifying the initial drop size in computational simulations of spray flows.

## MATHEMATICAL FORMULATION

The basic integral form of the conservation equations for mass, momentum, and energy has been shown in our previous work.<sup>20–22</sup> We present the equations here for the purpose of placing this work in context. We consider a control volume that envelops the spray including all its complex break-up and atomization mechanisms, as shown in Figure 1. The approach is to relate the mass, momentum, and energy of the spray at the injector exit, to those at a downstream location where the spray is fully atomized. Thus, we avoid the treatment of the complex atomization physics (usually expressed in partial “differential” equations), and attempt to find an “integral” relationship between the asymptotic states. The only main assumption in this formulation is that the liquid phase completes the transition from its initial state to a final state of fully atomized group of spherical droplets within the specified control volume, and that the viscous dissipation can be written in terms of known parameters such as the liquid velocity and dissipation length scale. Heat and mass transfer effects are not yet included, although it is not a far stretch of the current method to include them. For the control volume described above, the integral form of conservation equations of mass and energy for the liquid phase are as follows:

$$\rho_L u_{inj} A_{inj} = \int_{u=0}^{u_{max}} \int_{D=0}^{D_{max}} n \bar{p}(D, u) \frac{\pi D^3}{6} \rho_L u A dD du \approx \frac{\pi}{6} n \rho_L \bar{u} A \sum_i^N p(D_i) D_i^3 \Delta D_i, \quad (1)$$

$$\rho_L \frac{u_{inj}^3}{2} A_{inj} = \frac{\pi}{12} n \rho_L \bar{u}^3 A \sum_i^N p(D_i) D_i^3 \Delta D_i + n \bar{u} A \pi \sigma \sum_i^N p(D_i) D_i^2 \Delta D_i + K \mu_L \left\langle \left( \frac{\partial u}{\partial y} \right)^2 \right\rangle (Vol). \quad (2)$$

The mass conservation is achieved by equating the injected mass flow rate with the mass of the droplets contained in a volume swept by the average drop velocity,  $\bar{u}$ , over a spray area,  $A$ . The velocity distribution is simplified to an average drop velocity in Eqs. (1) and (2). The cross-sectional area,  $A$ , represents the physical extent of the spray at the plane where full atomization is achieved, which can be determined by the spray cone angle and the atomization length. The drop number

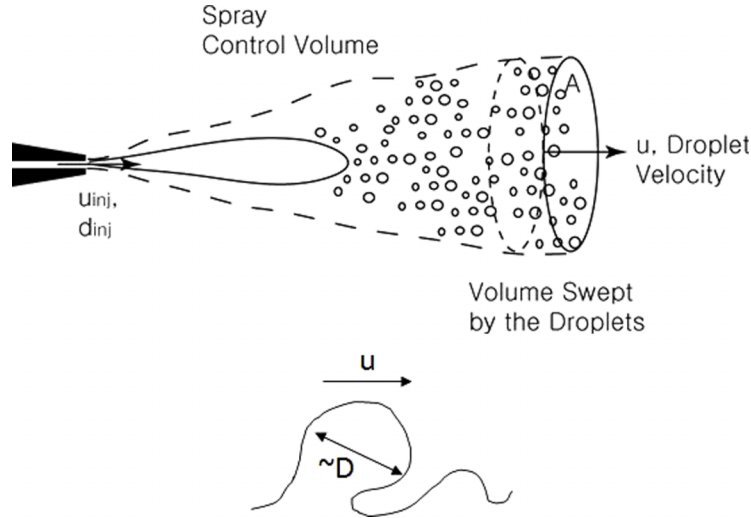


FIG. 1. The schematic of the spray control volume used for the integral analysis. The inset shows the reasoning for the viscous dissipation term in Eq. (3).

density is  $n$ , while  $\rho_L$  and  $D_i$  are the liquid density and droplet diameter, respectively.  $p(D_i)$  is the normalized drop size distribution, and  $\Delta D_i$  is the drop size bin width.

The liquid- and gas-phase momentum equations can be included in iterative numerical solutions,<sup>20–22</sup> which would involve the drop drag coefficient and effects of density of both gas (in the drag term) and liquid (in the momentum term). Such momentum effects have been discussed in length in one of our previous works.<sup>21</sup> As will be shown later, the current formulation is applicable to sprays in different configurations (e.g., swirl), as long as all the velocity components (axial and tangential for swirl sprays) are accounted for in the kinetic energy term.

Here, we focus on the SMD-velocity relationship, by using the mass (Eq. (1)) and energy balance (Eq. (2)). An estimate of the average viscous dissipation can be written as follows:

$$\mu_L \left\langle \left( \frac{\partial u}{\partial y} \right)^2 \right\rangle (SprayVolume) \sim \mu_L \left( \frac{u}{D_{32}} \right)^2 (SprayVolume). \quad (3)$$

Physically, the deformation of the spray liquid column toward droplets would occur at some velocity scale, which we will take to be the mean liquid velocity, and at the length scale of the droplets formed. Here, we take the length scale to be the SMD itself, since that is the scale at which the liquid deformation leading to droplet formation occurs, as depicted in Fig. 1 inset.  $K$  is the only adjustable constant in this formulation, as the exact relationship between the viscous dissipation terms and the spray volume is approximated. The dissipation term in our previous work<sup>20–22</sup> was only dimensionally correct and *ad hoc*. It led to some reasonable results, but also caused some numerical difficulties when the liquid velocity was large or close to the injection velocity. Now, the reason for this previous numerical instability is evident as shown below: when the liquid velocity approaches the injection velocity, the expected drop diameter is infinite (see Figure 2, for example). Schmehl<sup>29</sup> notes that for droplet breakup (secondary atomization) processes, the droplet viscous dissipation is exactly  $16\pi\mu R_o^3 \left( \frac{\dot{y}}{y} \right)^2$ , where  $R_o$  is the initial drop radius,  $y$  is the ellipsoid coordinate, and therefore  $dy/dt$  is the surface velocity. Eq. (3) is mathematically analogous to the expression of Schmehl,<sup>29</sup> where the ratio of the velocity to dissipation length scale is squared and then multiplied by a volume term and viscosity.

Substitution of Eq. (5) into the energy equation (Eq. (2)), after solving for  $n$  from Eq. (1),<sup>20–22</sup> gives us a quadratic equation for the  $D_{32}$ -velocity relationship,

$$\rho_L \left( \frac{u_{inj}^2 - \bar{u}^2}{2} \right) D_{32}^2 - 6\sigma D_{32} - K' \mu \bar{u}^2 = 0. \quad (4)$$

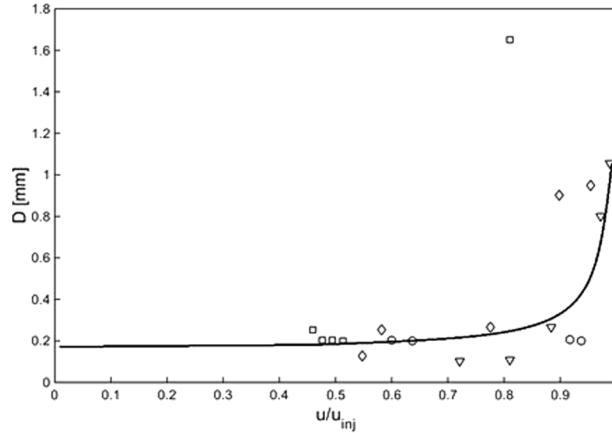


FIG. 2. Comparison of the calculated SMD with experimental data of Ruff and Faeth.<sup>26</sup>

$K'$  now absorbs the spray volume term, for simplicity. As will be discussed later (in Figures 7 and 8),  $K'$  increases with increasing distance from the injector, as the spray volume increases. This formulation becomes yet simpler for a fixed droplet diameter ( $D_{32} \rightarrow D$ ), which would allow for a transform of velocity to drop size distributions, as will be shown later. This leads to a quadratic solution for the  $D_{32}$ -velocity relationship,

$$D_{32} = \frac{3\sigma + \sqrt{9\sigma^2 + K' \rho_L \mu \bar{u}^2 \frac{u_{inj}^2 - \bar{u}^2}{2}}}{\rho L \frac{u_{inj}^2 - \bar{u}^2}{2}}. \quad (5)$$

The solution branch with the negative sign (before the square-root term) is discarded, due to its non-physical value.

## RESULTS AND DISCUSSION

A plot of Eq. (5) is shown in Figures 2 and 3, as solid lines, and comparison is made with experimental data for sprays without swirl (Figure 2) and with swirl (Figure 3). Figure 2 compares Eq. (5) with  $D_{32}$  vs. drop velocity data for pressure-atomized sprays with no swirl,<sup>26</sup> while Figure 3 is a comparison with the most probable drop size vs. the drop velocity obtained from joint-probability density function (pdf) data in swirl sprays.<sup>23</sup> The plots show that if the spray or

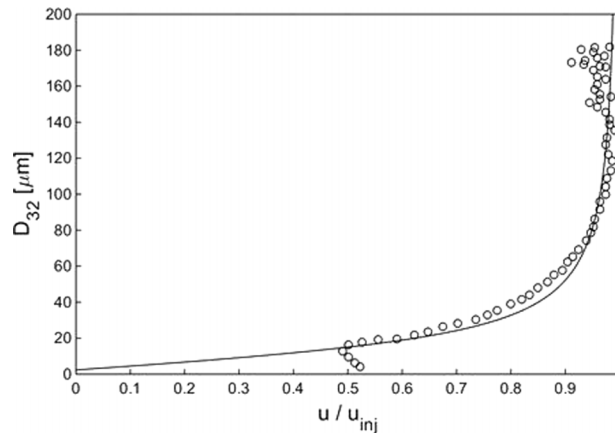


FIG. 3. Comparison of the calculated SMD with experimental data of Rimbert and Castanet.<sup>27</sup>

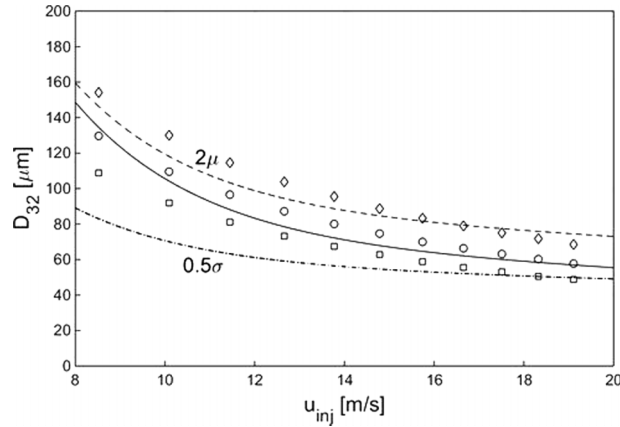


FIG. 4. Comparison of SMD with the correlations of Lefebvier,<sup>24</sup> for swirl sprays.

droplet velocity has not lost (converted) any of its kinetic energy to surface tension energy, i.e.,  $\bar{u} = u_{inj}$ , then the expected drop size is infinity. Physically, this means that no droplets exist, and that the liquid column is intact. As more of the initial kinetic energy is lost through fluid dynamic drag between the liquid and the gas, then the corresponding loss of kinetic energy must appear as surface energy, minus the viscous dissipation. Thus, when  $\bar{u} < u_{inj}$ , the resulting drop size is smaller. Below a certain range,  $\bar{u}/u_{inj} \approx 0.75$  for the pressure-atomized sprays without swirl in Figure 2, the decrease in the drop size is gradual with respect to the velocity decrease, meaning that a near “equilibrium” has been reached for the energy distribution in the spray. A later plot (Figure 4) will show that other parameters such as surface tension and viscosity result in expected trends for the drop size. Thus, the plots in these figures show that there is a “break-up” regime where the velocity of the liquid phase is not substantially different from the injection velocity and the drop size is very large or generation of small droplets improbable. The “atomization” regime is attained when the liquid-phase velocity has been retarded to a sufficient degree, and then the drop size change is relatively small for any further reductions in the drop velocity. The latter fact is useful for estimating the initial drop size in spray computations as the drop size is less sensitive to the exact value of liquid velocities at this range.

A correlation by Wu *et al.*<sup>30</sup> shows similar (but apparently reversed) asymptotic behavior with current results in Figures 2 and 3. The correlation gives  $SMD/d = 46.4/We^{0.74}$ ,<sup>30,31</sup> where the Weber number,  $We$ , is based on the jet speed. Thus this correlation gives infinite SMD at zero jet speed with a rapid decrease toward an asymptotic SMD at high jet speeds. We may reason that this is the same effect observed in our energy balance, where the jet speed is representative of the

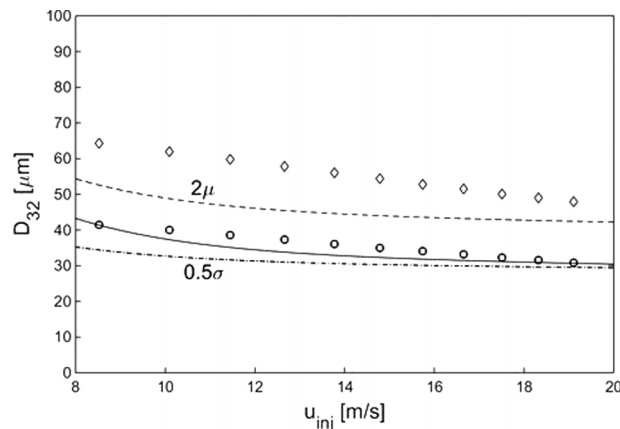


FIG. 5. Comparison with SMD with correlations of Chen *et al.*<sup>25</sup>

kinetic energy and zero Weber number corresponds to no kinetic energy available to be converted to surface energy, and therefore infinite drop size as in Figures 2 and 3. Figure 3 shows experimental data by Rimbert and Castanet,<sup>27</sup> who obtained detailed statistics of drop size and velocity in swirl sprays. The data shown in Figure 3 are the most probable drop size at a given liquid velocity, which illustrate the utility of Eq. (5) in swirl sprays so long as all the relevant velocity components are included in the kinetic energy term.

We can also compare Eq. (5) with existing correlations for SMD, as shown in Figures 4 and 5. The first correlation by Lefebvre<sup>24</sup> for swirl sprays contains the dependence on injection pressure (converted to the injection velocity), viscosity, and surface tension. The comparison is reasonable, where the mean spray velocity needs to be estimated in Eq. (5). Once a reasonable estimate is made, the values for both spray velocity and the constant,  $K'$ , are fixed. Increasing the viscosity results in larger drop size, and the decrease in the surface tension smaller drop size, where the decrease due to the latter effect is somewhat overestimated by Eq. (5). Another correlation by Chen *et al.*<sup>25</sup> includes the effect of the viscosity, but not surface tension. Equation (5) generates again favorable comparison, where the surface tension effect is still present but relatively small for the injection velocities of interest.

In computational fluid dynamics (CFD) of sprays, including spray evaporation and combustion, setting the initial conditions for the drop size and velocity has been the biggest hurdle in accurate simulations. Once the initial drop size and velocity are properly set, then there are several reliable methods for subsequent tracking of the particles, such as particle-in-cell (Eulerian-Lagrangian) calculations. Phase change, mass, and energy transfers can also be effectively treated using thermodynamic modules. Thus, a capability to specify the droplet initial conditions, based on the first principles, is of utmost necessity, to replace the *ad hoc* models presently used in many commercially available software packages. We start by taking note of the fact that the energy balance used in Eq. (5) can be used between any two locations. In Figure 1, we have applied the method from the injector exit to the “atomization plane,” where the liquid core has completely disintegrated and atomized into spherical droplets. In compact sprays, such as swirl sprays, this may be an ideal application since the spray initial conditions can be set at a location close to the injector exit. But what about pressure-atomized sprays without swirl, such as diesel sprays, with atomization lengths typically observed at  $x/d$  of 100–200<sup>1,2</sup> Much can happen within the volume that extends to such large axial locations, in terms of fuel mixing and combustion, for instance. Thus, it is necessary to set the initial conditions in a different manner.

If we again look at results in Figures 2 and 3, we can see that it is possible to use the velocity information to set the initial SMD, since the quadratic formula (Eq. (5)) provides a direct velocity-drop size relation. Also, from such plots, we can obtain estimates for the maximum and minimum drop size, to determine the general shape, variance term, of the drop size distribution. In this regard, we note that the liquid-phase velocities are quite accurately computed by computational

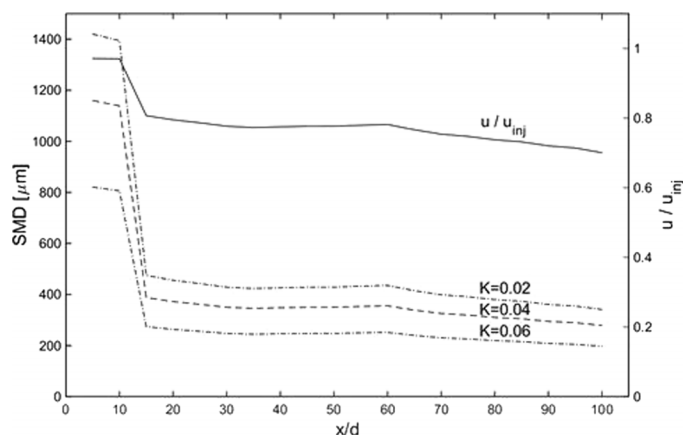


FIG. 6. SMD calculated from CFD-generated average liquid velocities. CFD is for a liquid jet, with no droplets in the flow.

methods. For example, Figure 6 shows the average liquid velocity as a function  $x/d$  for a liquid jet at injection velocity of 56 m/s, the same as the experiment by Ruff and Faeth.<sup>26</sup> Although the centerline velocity persists at a level close to the injection velocity to a large axial location, velocity averaged over the cross section of the liquid jet undergoes a transition to lower value much earlier, as seen in Figure 6. Thus, we can use this average liquid velocity to find the SMD's as a function of  $x/d$ , again using Eq. (5), which are overlaid in Figure 6 for various values of  $K$ . We can see that the initial SMD tends to be quite large, 800–1400  $\mu\text{m}$ , depending on  $K$ , and drops to 250–450  $\mu\text{m}$  range, when the average liquid velocity has been retarded by  $x/d \sim 15$ . Thus, we can use the SMD calculated using Eq. (5) at, say,  $x/d = 5$  to set the initial SMD. Subsequent computations of the spray flow to track drop motion and dispersions (that can cause variations in the SMD at axial and radial locations) show quite good agreement with data of Ruff and Faeth,<sup>26</sup> as shown in Figure 7. Figure 7 shows the CFD results for SMD along with drop velocity as a function of the radial location, as computed using initial SMD specified at  $x/d = 5$  and  $K' = 0.06$ . For initial SMD specification, only one value of  $K'$  is needed. However, for local SMD calculations,  $K'$  increases nearly linearly with  $x/D$  since it contains the spray volume term (Eq. (3)). These are compared with SMD measurements of Ruff and Faeth,<sup>26</sup> and again confirmed with Eq. (5) that relates the drop velocity with SMD at the same location. Although the initial SMD was set at a location close to the injector ( $x/d = 5$ ) in Figure 7 for comparison with data at  $x/d = 12.5, 25, 50,$  and  $100$ , for most simulations SMD initial condition should be set beyond  $x/d = 15$ , where the transition to the equilibrium liquid momentum and therefore SMD is achieved as shown in Figure 6. Some pertinent details of the computational work for the liquid velocity (Figures 6 and 8), spray CFD (Figure 7), and experimental data of Ruff and Faeth<sup>26</sup> are included in the Appendix.

Figure 7 shows the SMD remains high near the centerline, mainly because  $x/d$  locations are well below the so-called atomization length. Lower SMD are observed near the periphery of the spray, as smaller droplets preferentially disperse toward regions of lower velocity. This observation also points to a method for more spatially detailed specifications of the initial drop size. That is, instead of initiating the spray calculations at a plane ( $x/d = 5$  in the above example) close to the injector exit, we can specify the drop initial conditions at the spray “boundary layer,” which corresponds to the regions where atomization is taking place from the liquid surface in the pressure-atomized sprays. This will amount to a two-dimensional specification of the drop initial conditions, where the SMD and velocities are specified at the inner radial location (close to the liquid-air interface). We take the advantage of the fact that close to the injector, the liquid velocities (shown as dotted lines in Figure 7) tend to be independent of the drop size as the momentum is dominated by the initial inertia of the injection. The available liquid velocity can then be converted to local SMD as in Figure 7.

An alternative method for spatial specification of the initial drop size is to use the CFD results for axi-symmetric, columnar liquid jet (Figure 6) directly, at the same initial spray injection conditions (injection velocity, injector diameter, and liquid properties), and again use the velocity data from such simulations, as shown in Figure 8. We immediately see that the liquid velocity profiles are much more compact than the actual spray flow, since the liquid column does not spread out as much as the droplet-laden flow in Figure 7. However, the SMD values are again close to the experimental data,<sup>26</sup> albeit at smaller radial locations. Thus, we can “release” the droplets of the calculated SMD's at the inner spray at the CFD-generated liquid velocity vectors (axial and radial components) to provide the local initial droplet conditions in spray simulations.

As noted earlier, for a fixed drop size,  $D_{32}$  in Eq. (5) simply reduces to  $D$  as a function of drop velocity, providing essentially the cross correlation between the drop size and velocity. This can be used to construct the drop size distribution, in addition to the SMD. There are on-going works by other researchers<sup>28,30,31</sup> to determine the exact drop velocity distributions which may deviate from conventional clipped-Gaussian probability density function. For the purpose of demonstrating the transform from the drop velocity to drop size distributions, we take the simple clipped-Gaussian velocity distribution ( $f(u)$ ) and use Eq. (5) to determine the drop size distribution ( $g(D)$ ), as shown in Figure 9, through Eq. (5). Due to the asymptotic behavior for drop size as a function a liquid velocity, there is a shift toward smaller drop size and a long tail in the large drop size, which is the drop size distribution observed in sprays. For the velocity distribution (—) centered at a larger



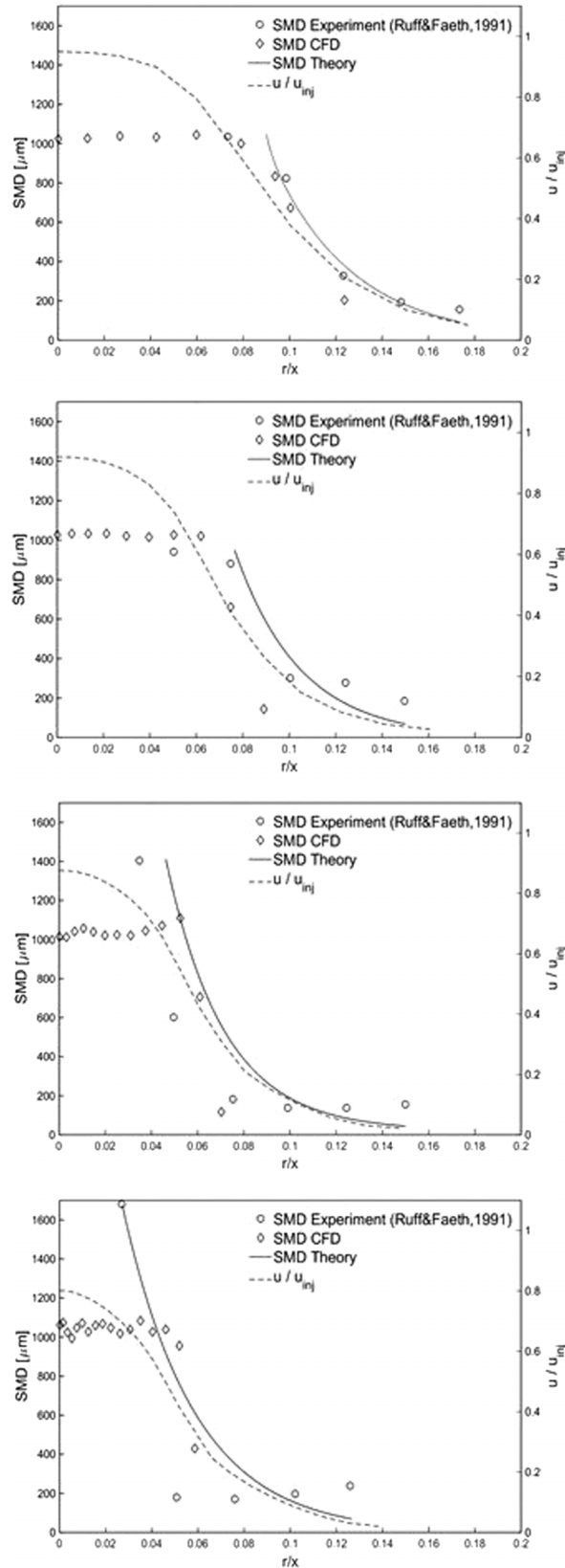


FIG. 7. Comparison of the SMD, measured, calculated, and also from CFD-generated liquid velocities. CFD is for a spray flow, with droplets released at  $x/d = 5$ . The plots are for  $x/d = 12.5$  (top), 25, 50, and 100 (bottom).

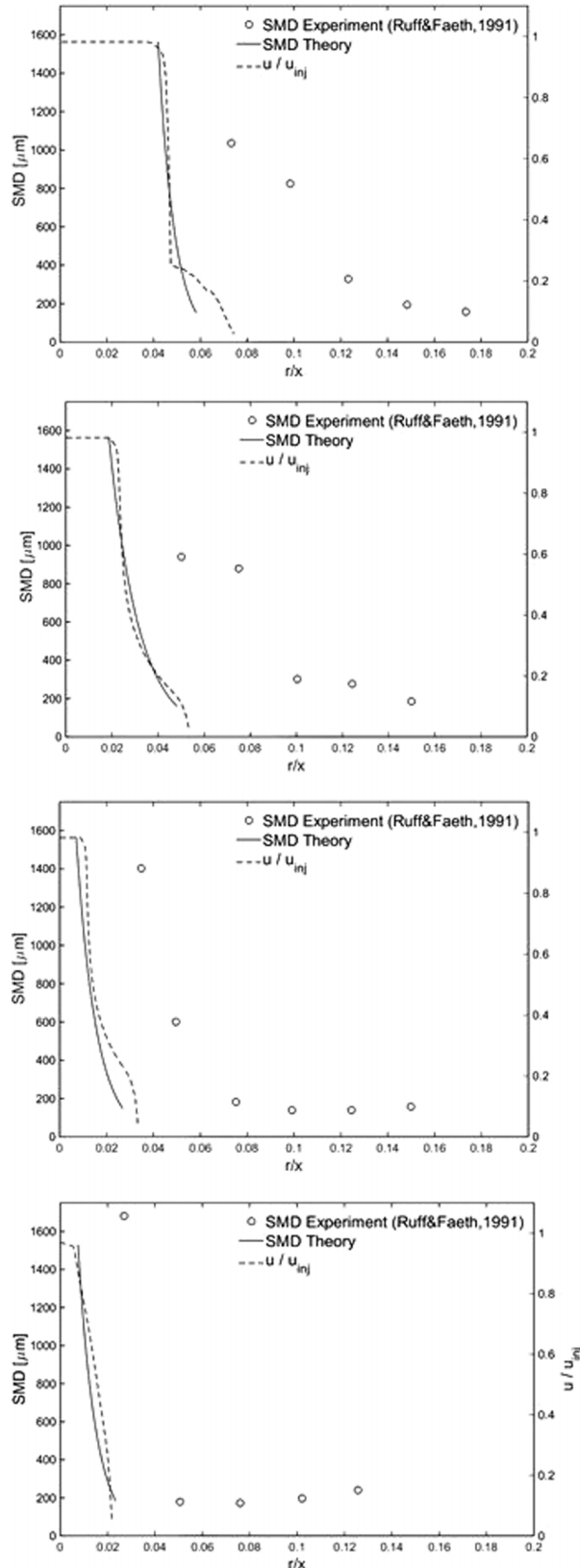


FIG. 8. Comparison of the SMD, measured, calculated, and also from CFD-generated liquid velocities. CFD is for a liquid jet, with no droplets in the flow. The plots are for  $x/d = 12.5$  (top), 25, 50 and 100 (bottom).

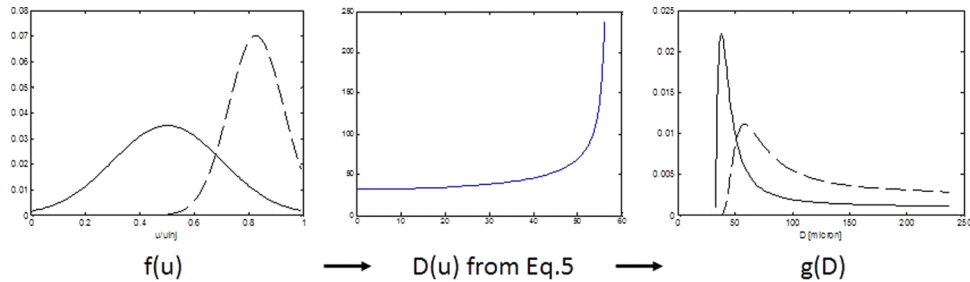


FIG. 9. Transform from velocity distributions to the drop size distributions via the “quadratic formula.”

liquid speed, the corresponding drop size distribution (—) is shifted toward larger drop size due to the steep slope of  $u$ - $D$  relationship near  $u_{inj}$ . When more exact velocity distributions are known from CFD or other means, then it can be easily converted to the drop size distribution using this approach.

## CONCLUSIONS

We have used a theoretical framework based on the integral form of the conservation equations, along with a phenomenological model of the viscous dissipation, to find a closed-form solution to the liquid atomization problem. The energy equation renders to a quadratic formula for the drop size as a function, primarily of the liquid velocity with surface tension and viscosity as fluidic parameters. The SMD found using the quadratic formula shows good agreement and physical trends, when compared with experimental observations. This approach also has good utility toward specifying initial SMD and drop size distributions in computational fluid dynamics of spray flows, either at plane close to the injector or more spatially at the spray boundary. The current method is based on the conservation of mass, energy, and also momentum, and therefore free of any non-physical assumptions. The only term to be modeled is the viscous dissipation (the Reynolds number effect); however, we have found a mathematically<sup>29</sup> and physically (Figure 1) reasonable form. There are quasi-DNS results on spray atomization<sup>27</sup> with which the only adjustable constant,  $K$ , in the current formulation can be evaluated. Also, further work may be needed in accurately specifying the spray “control volume,” since the current approach only links the initial and final asymptotic states. The “equilibrium” in liquid energy states should be reached since the energy terms to obtain Eq. (5) are prescribed based on the final drop kinetic and surface energy, along with the viscous dissipation that the liquid phase incurred during the atomization process.

## APPENDIX: DETAILS OF EXPERIMENTAL DATA USED AND COMPUTATIONAL WORK

For data of Ruff and Faeth,<sup>26</sup> water jets were injected vertically downward in still room air, using a 9.5-mm injector diameter, at a mean jet velocity of 56.3 m/s.<sup>26</sup> This corresponded to a mass flow rate of 3.99 kg/s, Reynolds number =  $Re = 534\,000$ , and Weber numbers based on gas and liquid densities of 500 and 412 000, respectively. The Ohnesorge number was 0.00 121. The liquid velocities were measured using a phase-discriminating laser Doppler velocimetry (LDV) system, which involved a conventional two-component LDV triggered by a 5-mW He-Ne laser to detect the presence of liquid in the probe volume. The drop size measurements were done via double-pulse holography, which were able to penetrate through the dense part of the sprays. Experimental uncertainties (95% confidence) for SMD measurements were less than 10%.<sup>26</sup>

For the simulations of liquid jet velocities used in Figures 6 and 8, the above injection conditions were used as the velocity inlet boundary condition in ANSYS/FLUENT (Version 16.2). Axisymmetric grid containing 108 883 quadrilateral cells was created using pre-processor ICEM software. The minimum and maximum face areas in the total domain are approximately  $7.4 \times 10^{-5} \text{ m}^2$  and  $9.3 \times 10^{-3} \text{ m}^2$  based on sensitivity analysis and standard wall functions are applied. Steady RANS equations for conservations of mass, momentum, and energy are solved in combination

with the realizable  $k$ - $\epsilon$  turbulence model by Shih *et al.*,<sup>32</sup> which predicts the spreading rate of both planar and round jets.<sup>33</sup> The SIMPLE algorithm is used in ANSYS/FLUENT for pressure-velocity coupling, while pressure interpolation is second order and second-order discretization schemes are used for both the turbulence kinetic energy term and the turbulence dissipation rate term of the equations.

For the spray simulations shown in Figure 7, a Lagrangian-Eulerian model is used, again in ANSYS/FLUENT. A full, three-dimensional “test section” grid of dimensions  $0.21 \text{ m} \times 0.21 \text{ m} \times 1.9 \text{ m}$  was made with the pre-processor ICEM software, with 333 036 hexahedral cells. A stretching ratio of 1.05 controls the cells located in the immediate surroundings of the nozzle. The Eulerian component was similar to the liquid jet simulations described in the previous paragraph. Lagrangian trajectory simulations are performed for the discrete phase. The discrete phase interacts with the continuous phase, and the discrete phase model source terms are updated after each continuous phase iteration. To solve the equations of motion for the droplets, the “automated tracking scheme selection” is adopted to be able to switch between higher order lower order tracking schemes. This mechanism can improve the accuracy and stability of the simulation.<sup>34</sup> SMD diameter as prescribed by Eq. (5) and Figure 6 is input as a Rosin-Rammler distribution, at 300 uniformly distributed points on the injector exit. The spherical drag law is used to estimate the drag coefficients. It assumes that the surface tension on the drop-fluid interface is strong enough to resist the tendency of the aerodynamic force to deform the drop. In this scenario, droplets are assumed to be non-deforming spheres, and drag coefficients ( $C_d$ ), as functions of the Reynolds number ( $Re$ ), are estimated based on experimental drag data for solid spheres. The correlation proposes the following drag coefficient for a wide range of Reynolds numbers up to  $5 \times 10^4$ :  $C_d = a_1 + \frac{a_2}{Re} + \frac{a_3}{Re^2}$  in which  $a_1$ ,  $a_2$ , and  $a_3$  are three constants that apply over several ranges of  $Re$  given by Morsi and Alexander.<sup>35</sup>

- <sup>1</sup> G. M. Faeth, “Structure and atomization properties of dense turbulent sprays,” in *23rd International Symposium on Combustion* (The Combustion Institute, 1990), pp. 1345–1352.
- <sup>2</sup> G. M. Faeth, L.-P. Hsiang, and P.-K. Wu, “Structure and break-up properties of sprays,” *Int. J. Multiphase Flow* **21**, 99–127 (1995).
- <sup>3</sup> W. E. Ranz, “Some experiments on orifice sprays,” *Can. J. Chem. Eng.* **36**, 175 (1958).
- <sup>4</sup> C. C. Miese, “Correlation of experimental data on disintegration of liquid jets,” *Ind. Eng. Chem.* **47**, 1960 (1955).
- <sup>5</sup> T.-W. Lee and A. Mitrovic, “Liquid core structure of pressure-atomized sprays via laser tomographic imaging,” *Atomization Sprays* **6**, 111–126 (1996).
- <sup>6</sup> E. Babinsky and P. E. Sojka, “Modeling drop size distributions,” *Prog. Energy Combust. Sci.* **28**, 303–329 (2002).
- <sup>7</sup> S. D. Sovani, P. E. Sojka, and Y. R. Sivathanu, “Prediction of drop size distributions from first Principles: Joint pdf effects,” *Atomization Sprays* **27**, 213–222 (2002).
- <sup>8</sup> R. W. Sellens and T. A. Brzustowski, “A simplified prediction of the drop size distribution in a spray,” *Combust. Flame* **65**, 273–279 (1986).
- <sup>9</sup> X. Li and R. S. Tankin, “Drop size distribution: A derivation of a Nukiyama-Tanasawa type distribution function,” *Combust. Sci. Technol.* **60**, 345–357 (1988).
- <sup>10</sup> X. Li, L. P. Chin, R. S. Tankin, T. Jackson, J. Stutrud, and G. Switzer, “Comparison between experiments and predictions based on maximum entropy for sprays from a pressure atomizer,” *Combust. Flame* **86**, 73–89 (1991).
- <sup>11</sup> C. W. M. van der Geld and H. Vermeer, “Prediction of drop size distributions in sprays using the maximum entropy formalism: The effect of satellite formation,” *Int. J. Multiphase Flow* **20**(2), 363–381 (1994).
- <sup>12</sup> M. Ahmadi and R. W. Sellens, “A simplified maximum-entropy-based drop size distribution,” *Atomization Sprays* **3**, 291–310 (1993).
- <sup>13</sup> J. Cousin, S. J. Yoon, and C. Dumouchel, “Coupling of classical linear theory and maximum entropy formalism for prediction of drop size distribution in sprays: Application to pressure swirl atomizers,” *Atomization Sprays* **6**, 601–622 (1996).
- <sup>14</sup> C. Dumouchel and S. Boyaval, “Use of the maximum entropy formalism to determine drop size distribution characteristics,” *Part. Part. Syst. Charact.* **16**, 177–184 (1999).
- <sup>15</sup> C. Dumouchel, “A new formulation of the maximum entropy formalism to model liquid spray drop-size distribution,” *Part. Part. Syst. Charact.* **23**, 468–479 (2006).
- <sup>16</sup> W. A. Sirignano and C. Mehring, “Review of theory of distortion and disintegration of liquid streams,” *Prog. Energy Combust. Sci.* **26**, 609–655 (2000).
- <sup>17</sup> M. R. Archambault, C. F. Edwards, and R. W. MacCormack, “Computation of spray dynamics by moment transport equations. II. Application to calculation of a quasi-one dimensional spray,” *Atomization Sprays* **13**(1), 89–115 (2003).
- <sup>18</sup> M. R. Archambault and C. F. Edwards, “Computation of spray dynamics by direct solution of moment transport equations-inclusion of nonlinear momentum exchange,” in *Eighth International Conference on Liquid Atomization and Spray Systems, Pasadena, CA, USA, July 2000* (ILASS, 2000).
- <sup>19</sup> S. Subramaniam, “Statistical representation of a spray as a point process,” *Phys. Fluids* **12**(10), 2413–2431 (2000).
- <sup>20</sup> T.-W. Lee and D. Robinson, “A method for direct calculations of the drop size distribution and velocities from the integral form of the conservation equations,” *Combust. Sci. Technol.* **183**(3), 271–284 (2011).

- <sup>21</sup> T.-W. Lee and J. Y. Lee, "Momentum effects on drop size, calculated using the integral form of the conservation equations," *Combust. Sci. Technol.* **184**, 434–443 (2012).
- <sup>22</sup> T.-W. Lee and J. H. Ryu, "Analyses of spray break-up mechanisms using the integral form of the conservation equations," *Combust. Theory Model.* **18**(1), 89–100 (2014).
- <sup>23</sup> N. Rimbert and G. Castanet, "Liquid atomization out of a full cone pressure swirl nozzle," personal communications (2015).
- <sup>24</sup> A. H. Lefevbre, *Atomization and Sprays* (Hemisphere Publishing Corp., 1989).
- <sup>25</sup> L. Chen, Z. Liu, P. Sun, and W. Huo, "Formulation of a fuel spray SMD model at atmospheric pressure using design of experiments," *Fuel* **153**, 355–360 (2015).
- <sup>26</sup> G. Ruff and G. M. Faeth, "Structure of the near-injector region of nonevaporating pressure-atomized sprays," *J. Propul. Power* **7**, 221–231 (1991).
- <sup>27</sup> M. Gorokhovski and M. Herrmann, "Modeling primary atomization," *Annu. Rev. Fluid Mech.* **40**, 343–366 (2008).
- <sup>28</sup> P. Marmottant and E. Veillermaux, "On spray formation," *J. Fluid Mech.* **498**, 73–111 (2004).
- <sup>29</sup> R. Schmehl, "Advanced modeling of droplet deformation and breakup for CFD analysis of mixture preparation," ILASS-Europe, 2002.
- <sup>30</sup> P. K. Wu, R. F. Miranda, and G. M. Faeth, "Effects of initial flow conditions on primary break-up of nonturbulent and turbulent liquid jets," AIAA Paper No. 94-0561, 1994.
- <sup>31</sup> S. S. Yoon and S. D. Heister, "A nonlinear atomization model based on a boundary layer instability mechanism," *Phys. Fluids* **16**, 47–61 (2004).
- <sup>32</sup> T.-H. Shih, W. W. Liou, A. Shabbir, Z. Yang, and J. Zhu, "A new  $k-\epsilon$  eddy viscosity model for high Reynolds number turbulent flows," *Comput. Fluids* **24**, 227–238 (1995).
- <sup>33</sup> ANSYS, Inc., ANSYS Fluent 12.0 User's Guide, 2009.
- <sup>34</sup> S. Subramaniam, "Lagrangian–Eulerian methods for multiphase flows," *Prog. Energy Combust. Sci.* **39**, 215–224 (2013).
- <sup>35</sup> S. A. Morsi and A. J. Alexander, "An investigation of particle trajectories in two-phase flow systems," *J. Fluid Mech.* **55**, 193–208 (1972).